COMMUNICATIONS PHYSICS

ARTICLE

DOI: 10.1038/s42005-018-0088-2 OPEN

Orbital angular momentum dichroism in nanoantennas

R.M. Kerber [1,2], J.M. Fitzgerald[2], S.S. Oh [2,3], D.E. Reiter[1,2,4] & O. Hess [2]

When light interacts with matter, dichroism with respect to the handedness of circularly polarized light is well established. But what happens if the light further possesses an orbital angular momentum? In this paper, we discuss possible definitions of orbital angular momentum dichroism and define a new type of dichroism, the class dichroism. By numerically calculating the scattering cross-section spectra, we study the dichroism of a plasmonic nanostructure interacting with orbital angular momentum light. By considering the exemplary case of twisted, stacked nanorods, we show that the orbital angular momentum dichroism can be as strong as dichroism induced by circular polarization. We present a detailed classification of the different types of orbital angular momentum dichroism, which paves the way for new chiroptic spectroscopic techniques.

[1] Institut für Festkörpertheorie, Universität Münster, Wilhelm-Klemm-Straße 10, 48149 Münster, Germany. [2] Department of Physics, Imperial College London, Prince Consort Road, London SW7 2AZ, UK. [3] School of Physics and Astronomy, Cardiff University, The Parade, Cardiff CF24 3AA, UK. [4] Center for Multiscale Theory and Computation, Universität Münster, Corrensstraße 40, 48149 Münster, Germany. Correspondence and requests for materials should be addressed to R.M.K. (email: r.kerber@wwu.de) or to O.H. (email: o.hess@imperial.ac.uk)

Light can be characterized by its polarization state, for example by the left- and right-handed circular polarization, also denoted as spin angular momentum (SAM). Depending on its polarization, the interaction of light with certain materials can be different, resulting in a helicity-dependent absorption or scattering. This dichroic response is often defined as the difference in absorption or scattering for excitations of different handedness of circular polarization. While the well-established term circular dichroism (CD) is used for the difference in absorption, the difference in scattering is denoted with circular differential scattering (CDS)[1–3]. On the nanoscale, CD and CDS occur typically for chiral objects, i.e., objects which cannot be superimposed onto their mirror image, like molecules, DNA and other chemical or biomolecular chiral substances[4–6] and has been studied for many different types of plasmonic nanostructures like chiral single particles, chiral nanoparticle assemblies and chiral metamaterials[7–14] showing a strongly enhanced dichroism compared to natural substances[15,16].

In addition to the circular polarization states, light can also carry orbital angular momentum (OAM), which has emerged as a characteristic to classify light[17,18] and is used for information encoding[19–21]. For OAM light, the interaction with matter differs significantly compared to plane waves. For single particles, like atoms, molecules or quantum dots, the interaction can drive unusual transitions[22–27] which are dipole forbidden. The OAM of light is not restricted to only two states, but in principle extends to infinite values. Similar to the circular polarization, the OAM can take positive and negative values. This leads to the immediate question: can we also define an orbital angular momentum dichroism? When defining dichroism for OAM light, one has to be mindful of the fact that the circular polarization, characterized by its handedness s, and the OAM of light, quantizied by ℓ are strongly intertwined; in particular, one can distinguish two distinct classes, the parallel class for ℓ and s having same signs and the anti-parallel class for ℓ and s having opposite signs[22]. In the usual definition, dichroism describes the difference of two kinds of beams. It is indeed not a trivial task to define dichroism for OAM light because it offers multiple possible combinations of SAM and OAM.

In this paper, after an introduction of a mathematical framework for OAM light, we discuss how to classify the dichroism for OAM light beams. As an example we will then study the dichroism occurring in plasmonic nanoantennas. As a testbed we chose stacked nanorods, which have been shown to display a strong and tunable dichroic response to circularly polarized light[28–33]. In particular, we ask the question whether a dichroism for OAM light can be readily observed for these nanostructures. We study whether a dichroism emerges for the same handedness of polarization and how the dichroism relates to OAM. We find that for rotationally arranged nanoparticles different kinds of dichroism emerge for different combinations of values of the SAM and OAM of light.

Results

OAM light. In contrast to plane waves, an OAM light beam carries an additional phase, which is associated with the formation of a vortex or phase singularity at the beam axis. Because of the helical phase front of an OAM beam, such light is also called twisted light. The properties of an OAM light beam can be quantified by its handedness of circular polarization denoted by $s = \pm 1$ and its value of OAM given by $\ell = 0, \pm 1, \pm 2, \ldots$; the latter being also called topological charge. We emphasize that—in contrast to s—the OAM ℓ is not restricted to two values.

Mathematically OAM light can be described by the vector potential **A** Here we describe a monochromatic Bessel beam with frequency ω in Cartesian coordinates $\{x, y, z\}$ by $\mathbf{A}(\mathbf{r},t) = (A_x e_x + A_y e_y + A_z e_z)\exp[-i(\omega t - q_z z)]$, propagating along the z-axis with the wave vector q_z. The components of the vector potential are[22,34,35]:

$$A_x(\mathbf{r}, t) = A_0 J_\ell(q_r r) exp(i\ell\varphi), \quad (1)$$

$$A_y(\mathbf{r}, t) = isA_0 J_\ell(q_r r)\exp(i\ell\varphi), \quad (2)$$

$$A_z(\mathbf{r}, t) = -is\frac{q_r}{q_z} A_0 J_{\ell+s}(q_r r) exp(i(\ell + s)\varphi), \quad (3)$$

with radius $r = \sqrt{x^2 + y^2}$, azimuthal angle $\varphi = \arctan(y/x)$, q_r the wave vector in the transversal plane and A_0 the amplitude. $J_\ell(q_r r)$ is the Bessel function of order ℓ. We employ Bessel beams, because they are exact solutions of Maxwell's equations[36]. We use a fixed ratio of $q_r/q_z \approx 1.6$ to result in a highly focussed beam with a diameter of the first maximum of a twisted light beam with $\ell = 1$ of 1 μm. The corresponding field patterns can be found, e.g., in ref. [37].

Looking at the vector potential we can clearly identify the additional phase factor $\exp(i\ell\varphi)$ in the components, which then gives rise to the OAM of the light. We also see that the beam are classified by the SAM s and we note that distinct field patterns appear for different combinations of ℓ and s. This leads to the classification of OAM light into two distinct classes of light, called the parallel and anti-parallel class. In the parallel class the signs of ℓ and s are the same, while in the anti-parallel class they are opposite. The field profiles and behaviour of the two classes are fundamentally different and they do not evolve into each other in time[22].

Definitions of dichroism. While dichroism has been widely studied in terms of circularly polarized excitation, only few studies of dichroism for OAM light are available. For example, OAM light enables the possibility to create a dichroic response in non-chiral plasmonic nanostructures. When shining OAM light onto a hole in a metallic plane a circular dichroic response has been reported[38]. A further example is the angular momentum-dependent transmssion of vortex beam through plasmonic coaxial nanorings[39]. In contrast, for a polymer (which is a chiral molecule) no dichroic response was found[40,41]. When the description of OAM light-matter interaction includes higher order interactions[23], the electric quadrupole interactions cause a significant chiroptical response influenced by both the circular polarization and orbital angular momentum[42]. By using plasmonic nanoparticle aggregates, which show strong quadrupole fields, a discrimination of enantiomers becomes possible with OAM light[43]. In analogy to CD and CDS, which are caused by SAM, these studies thus demonstrate the necessity to define a new type of dichroism originating from the OAM.

For plane waves, CDS is defined as the scattering intensity difference between right handed ($s = 1$) and left handed ($s = -1$) beams when interacting with matter. In this paper, we will consider as a figure of merit the scattering cross-section $\sigma_{\ell,s}$ from a plasmonic nanostructure excited with different kinds of Bessel beams characterized by SAM s and OAM ℓ. For beams with $\ell = 0$, we recover plane waves and the CDS is well-defined via

$$\Delta\sigma^{\mathrm{CDS}} = \sigma_{0,+1} - \sigma_{0,-1}. \quad (4)$$

This definition of dichroism can be readily generalized to OAM light, where we keep ℓ fixed and just vary s. We name this

dichroism SAM-D defined as

$$\Delta\sigma_{\ell}^{\mathrm{SAM-D}} = \sigma_{\ell,+1} - \sigma_{\ell,-1}. \quad (5)$$

The CDS is regained for the special case of $\ell = 0$, i.e., $\Delta\sigma_{0}^{\mathrm{SAM-D}} = \Delta\sigma^{\mathrm{CDS}}$. The definition of dichroism for OAM light becomes much more complex, however, when we allow ℓ to vary. In fact, for OAM light the definition of dichroism is non-trivial because of the multiple combinations of SAM and OAM. A straightforward definition of OAM dichroism is to fix the handedness of the polarization s and the absolute value of ℓ and only allow the sign of OAM to vary. We call this dichroism OAM-D defined as

$$\Delta\sigma_{|\ell|,s}^{\mathrm{OAM-D}} = \sigma_{+|\ell|,s} - \sigma_{-|\ell|,s}. \quad (6)$$

In a more generalized definition of OAM dichroism the absolute value of OAM could vary. As an example, we could change the OAM by one and take the difference $\sigma_{|\ell|+1,s} - \sigma_{|\ell|,s}$. But at the beam axis, where the interaction with the plasmonic nanostructure is most relevant, the intensity of the beam is proportional to $r^{2|\ell|}$ and the light–matter interaction will be most likely dominated by the different intensity profiles of the beams with different $|\ell|$. Hence, we do not consider a generalized definition using OAM light with different absolute values of $|\ell|$.

Both the SAM-D and the OAM-D compare the scattering intensities of beams of different classes, e.g., the OAM-D $\Delta\sigma_{1,1}^{\mathrm{OAM-D}} = \sigma_{+1,+1} - \sigma_{-1,+1}$ includes one beam of the parallel class $\sigma_{+1,+1}$ and one of the anti-parallel class $\sigma_{-1,+1}$. When reversing the propagation direction of an OAM light beam, we find that both SAM and OAM should be inverted, hence, under inversion the class of the beam is conserved. Therefore, it is reasonable to define a new type of dichroism relying on the two classes of OAM light, i.e., the parallel and anti-parallel class. This definition has the further advantage that the intensity profiles, including the longitudinal components, remain the same (cf. Eq. (3)), while the intensity profile of the transverse component of the light fields is the same also in the SAM-D and OAM-D. We accordingly define a new dichroism called the class-D. For the parallel class (PC), we define

$$\Delta\sigma_{|\ell|}^{\mathrm{PC-D}} = \sigma_{|\ell|,+1} - \sigma_{-|\ell|,-1} \quad (7)$$

and for the anti-parallel class (APC) as

$$\Delta\sigma_{|\ell|}^{\mathrm{APC-D}} = \sigma_{-|\ell|,+1} - \sigma_{|\ell|,-1}\,. \quad (8)$$

As an example, the PC-D for $\ell = \pm 1$ is $\Delta\sigma_{1}^{\mathrm{PC-D}} = \sigma_{+1,+1} - \sigma_{-1,-1}$ including the two beams of the parallel class. The class-D compares the two beams with opposite propagation directions and, therefore, is the most similar one to the dichroism induced by circularly polarized light, which also can be understood as two beams with different propagation directions.

It is interesting to note that definitions of dichroism between the two classes can be derived by combining the definitions of the SAM-D and the OAM-D. As we argued above, we keep $|\ell|$ fixed to compare beams with the same intensity profiles. Already for ℓ being fixed we have six different possibilities to define a dichroism which are now covered by our definitions (two within the SAM-D, two for the OAM-D and two for the class-D).

Interaction with a plasmonic nanoantenna. To study the OAM related dichroism, we choose a design consisting of stacked nanoantennas which are composed of two identical

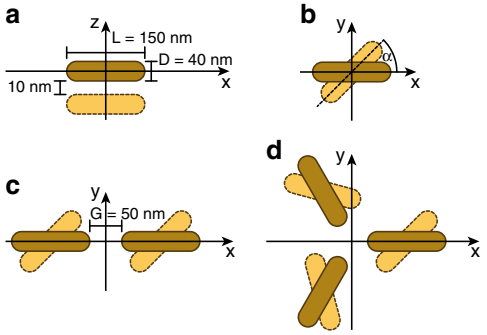

Fig. 1 Geometry of the plasmonic nanostructures. Single element nanoantenna consisting of two nanorods in *x*–*z* plane (**a**) and in *x*–*y* plane (**b**). Geometry of the dimer (**c**) and trimer (**d**) nanoantenna consisting of two and three elements, respectively

nanorods[28–33]. Each rod has a length of $L = 150$ nm and a circular cross-section with a diameter of $D = 40$ nm, while the ends of the rods are rounded by hemispheres. The upper rod lies in the $z = 0$ plane and the lower one is shifted down, forming a gap of 10 nm between both rods. By twisting the rods against each other around the z-axis, quantified by the angle α, the nanostructure obtains a chiral character. It is noteworthy that the twist angle of the rods can be experimentally adjusted by using reconfigurable DNA origami template and adding specifically designed DNA fuel strands to switch between different configuration[28,44,45]. Figure 1 shows a sketch of the geometry for a single element (a), (b) and of nanostructures consisting of two (c) and three elements (d).

We assume the antennas to be made of gold and surrounded by air. To numerically calculate the scattering cross-section of the nanoantennas, we use a boundary element method (BEM)[46] with experimental data for the dielectric function of gold[47].

In the following parts, we discuss what kinds of dichroism appear, when an OAM light beam interacts with a nanostructure. We start by focusing on a single element of stacked nanorods, a monomer (Fig. 1a, b), which has been shown to exhibit dichroism for circularly polarized light[28] and probe, whether we see the other types of dichroism in this structure excited by OAM light. Subsequently, we then investigate structures composed of several stacked elements, particularly in the $N = 2$ (dimer, Fig. 1c) and the $N = 3$ (trimer, Fig. 1d) configurations.

Monomer. For the single element ($N = 1$), we consider one pair of stacked rods as sketched in Fig. 1a, b and assume the OAM light to be incident on the nanoantenna from the bottom and aligned with the rotation axis of the nanostructure with the beam axis. The scattering cross-section and CDS for a single element $N = 1$ are shown in Fig. 2. A characteristic scattering cross-section spectrum is displayed in Fig. 2a for $\ell = 0, \pm 1$ and $s = \pm 1$ considering a nanostructure with a rotation angle of $\alpha = 45°$. All spectra are normalized to the maximum value for $\ell = 0$ and $s = +1$. The spectrum shows a strong difference in intensities for the circularly polarized light ($\ell = 0$) at the resonance $\lambda_a = 710$ nm (dotted black vertical line), indicating a considerable dichroism. We further observe a shoulder for $\ell = 0$ and $s = -1$ at $\lambda_b = 770$ nm. From the surface charge distribution (the inset of Fig. 2a), we can clearly distinguish both modes, because the sign of surface charge in the lower rod is different. These two resonances, which originate from the small distance between the two stacked rods, can be explained by the hybridization model[48] and are called anti-bonding and bonding mode, respectively[31]. To quantify the CDS, we plot $\Delta\sigma^{\mathrm{CDS}}$ in Fig. 2b for various angles $\alpha = 0°$ to 90°. For $\alpha = 0°$ (light red solid line) and

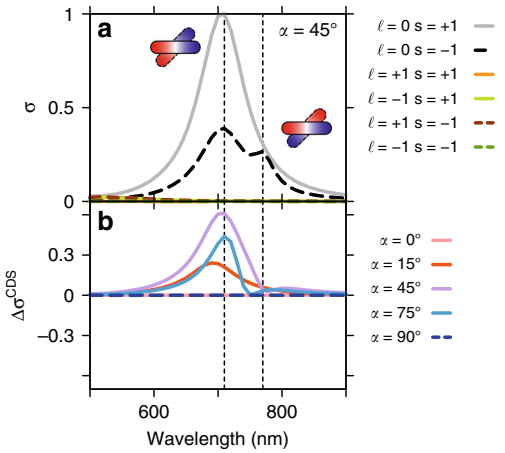

Fig. 2 Dichroism in the monomer. Scattering cross-section $\sigma_{\ell,s}$ for an angle $\alpha = 45°$ for different types of Bessel beams as indicated (**a**) and circular differential scattering $\Delta\sigma^{\mathrm{CDS}}$ for different angles α (**b**)

$\alpha = 90°$ (dark blue dashed line) there is no dichroism, because the nanostructure is not chiral. As soon as a little twist is introduced ($\alpha \neq 0°, 90°$), the structure becomes chiral and a dichroism occurs at the resonance wavelength, with the highest dichroism appearing at $\alpha = 45°$ (purple solid line). For angles $\alpha > 90°$ (not shown here) the sign of the dichroism changes because the rods are twisted in opposite direction, so that $\Delta\sigma^{\mathrm{CDS}}$ is simple the mirror image respective to the wavelength axis.

Next we consider an OAM beam with $\ell = \pm 1$. From the spectra in Fig. 2a we see that the scattering cross-section is three orders of magnitude lower in comparison to $\ell = 0$ and even in a zoom-in graph, we cannot see that a resonance is excited. For the monomer the interaction with the light field is weak, because the center of the rods are aligned with the beam axis where the intensity vanishes. Accordingly, no dichroism appears for OAM light (not shown) for such a configuration.

Dimer. Next, we consider a nanostructure design consisting of two elements with a gap which is aligned with the vortex of the OAM light beam, and each element is twisted in the same direction by the angle α as shown in Fig. 1c. Such a structure avoids the vortex with its vanishing electric field intensity and has been studied previously and shown to have an OAM dependent response to twisted light[37]. Before considering the OAM light, we check, if such a structure also exhibits a CDS. For this, we focus on the scattering cross-section for a beam with $\ell = 0$ impinging on the dimer in Fig. 3a. In the scattering cross-section, exemplarily shown for $\alpha = 45°$, we find two distinct resonance wavelengths at $\lambda_a = 730$ nm and $\lambda_b = 780$ nm belonging to the anti-bonding and bonding mode within each element. At both resonances, we find a difference in intensity, showing that also the dimer nanostructure exhibits dichroism, where a stronger intensity difference is found at λ_a. This is quantified in Fig. 3b, showing a similar behaviour to the monomer with no dichroic response found for $\alpha = 0,90°$ and the strongest dichroism found at $\alpha = 45°$.

Now we study the OAM dependent dichroic behaviour of the dimer. Using our example with stacks having a twist angle of $\alpha = 45°$, the scattering cross-section for OAM light with all combinations of $\ell = \pm 1$ and $s = \pm 1$ is shown in Fig. 3c. A different resonance mode is excited at $\lambda_d = 690$ nm. This is a dark mode resulting from the out-of-phase oscillation of the surface charges between the two elements[37]. Within each element the anti-bonding mode is excited. For the dark mode we observe a difference in intensity for different signs of circular polarization

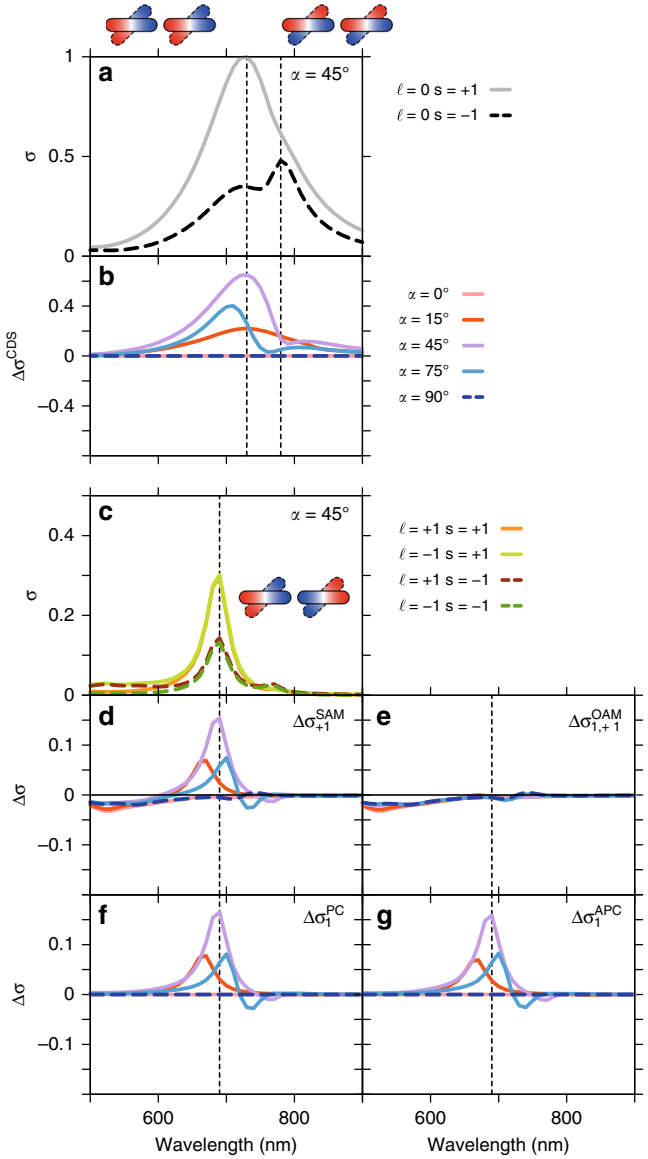

Fig. 3 Dichroism in the dimer. Scattering cross-section spectrum for an angle $\alpha = 45°$ for beams with $\ell = 0$ and $s = \pm 1$ (**a**) and circular differential scattering $\Delta\sigma^{\mathrm{CDS}}$ (**b**). Scattering cross-section spectrum for an angle $\alpha = 45°$ for Bessel beams with $\ell = \pm 1$ and $s = \pm 1$ (**c**). Spectra of several dichroisms as indicated: spin angular momentum (SAM) dichroism $\Delta\sigma_{+1}^{\mathrm{SAM-D}}$ for $\ell = 1$ (**d**), the orbital angular momentum (OAM) dichroism $\Delta\sigma_{1,+1}^{\mathrm{OAM-D}}$ for $s = +1$ (**e**), and the class dichroisms for the parallel class $\Delta\sigma_{1}^{\mathrm{PC-D}}$ (**f**) and the anti-parallel class $\Delta\sigma_{1}^{\mathrm{APC-D}}$ (**g**)

hinting towards a dichroism. We note that at $\lambda = 770$nm a very small peak is visible, which corresponds to the dark mode with the bonding mode within each element.

We begin by checking if we have a dichroism regarding the SAM (note that this is the generalization of the CDS) by plotting $\Delta\sigma_{+1}^{\mathrm{SAM-D}}$ (Eq. (5)) for $\ell = +1$ in Fig. 3d. Indeed, we find that we have a non-zero dichroism $\Delta\sigma_{+1}^{\mathrm{SAM-D}}$ with its maximal value for $\alpha = 45°$ at resonance wavelength of almost 15%. Because dichroism response distinguishes between different states of polarization, we infer that the circular polarization dichroism found for normal beams translates in this case directly to OAM beams, but with the dark mode taking the place of the bright mode. We note that for $\alpha = 0°,90°$ there is a small dichroism visible, which indicates that also the OAM plays a role.

Next, we quantify the dichroism regarding OAM by $\Delta\sigma_{1,+1}^{\mathrm{OAM-D}}$ (Eq. (6)) for $|\ell| = 1$ and $s = +1$ in Fig. 3e. We indeed find some small dichroism for different values of OAM, but it is one order of magnitude weaker than the effect of the SAM, except for $\alpha = 0°$ and $\alpha = 90°$. We further note that the line shape is not symmetric with respect to the wavelength-axis for two associated angles, for example $\alpha = 15°$ and 165° are no mirror images. This is not surprising because OAM light can induce a dichroism in non-chiral nanostructures[38].

We finish our discussion of the dimer case by considering the class dichroism (see Eq. (7) and Eq. (8)) in Fig. 3f, g. Here, we find a dichroism in the same order of magnitude than the SAM-D. Indeed, when looking at the definition of the class dichroism, always a change of sign of s is involved causing the class dichroism observed here. One difference, however, is that here for $\alpha = 0°$ and 90° indeed the dichroism vanishes completely.

In conclusion for the dimer we find dichroism for OAM light and the SAM-Dichroism is the strongest among the three types of dichroism.

Trimer. In the last example we increase the number of elements to $N = 3$, the trimer as sketched in Fig. 1d. The corresponding results of the scattering cross-section are displayed in Fig. 4.

Again we first check that the trimer also has a CDS by considering the spectrum of the scattering cross-section for circularly polarized light shown in Fig. 4a for a twist angle of $\alpha = 45°$. Two resonances at $\lambda_a = 730$nm and at $\lambda_b = 790$nm (left and right dotted vertical line) emerge, which belong to different configurations of surface charge and can roughly be classified as anti-bonding and bonding mode within each element. Like in the previous cases of the monomer and the dimer, a dichroic response is present. It is quantified in Fig. 4b with the largest dichroism appearing for $\alpha = 45°$.

When considering OAM light in Fig. 4c, the anti-parallel beams with $\ell = -s$ excite mainly the dark mode of the trimer occuring at $\lambda_d = 660$ nm, while the parallel beams with $\ell = s$ excite the bright mode of the trimer similar to the plane waves, which are split into bonding and anti-bonding mode. Due to the symmetry of the OAM light field determined by SAM and OAM and the discrete rotation symmetry of the trimer, this nanostructure with its three arms is able to distinguish between the two classes of twisted light[37]. However the resonances are not clearly resolved due to the complex structure of the trimer. The spectrum already indicates that due to the different resonance behaviour, an OAM induced dichroism is present for such a structure.

Now we study the different dichroisms as defined in Eqs. (5)–(8) in detail in Fig. 4d–g. We find a pronounced dichroic behaviour regarding the SAM shown by $\Delta\sigma_1^{SAM-D}$ of the order of 10–15%. Also for the OAM dichroism we now see a pronounced behaviour of the same order of magnitude. Note that the OAM-dichroism here is of same magnitude as the usual CDS. We further note, that both dichroisms behave quite similarly within the spectrum. Around the dark mode, they are negative, while for the bright mode the values are positive.

To further analyze the dichroism we look at the parallel (f) and anti-parallel class dichroism (g). Here, the two dichroisms for SAM and OAM partially cancel. For angles $\alpha \approx 45°$ we still see a strong dichroism, but mostly at higher wavelengths, which is a combined effect from SAM and OAM. Further, we find that for $\Delta\sigma_1^{\mathrm{PC-D}}$ the dichroism is positive, while for $\Delta\sigma_1^{\mathrm{APC-D}}$ it is negative, indicating the strong influence of the OAM induced dichroism.

We note that the trimer behaves fundamentally different to the dimer. This can be traced back to the higher number of available

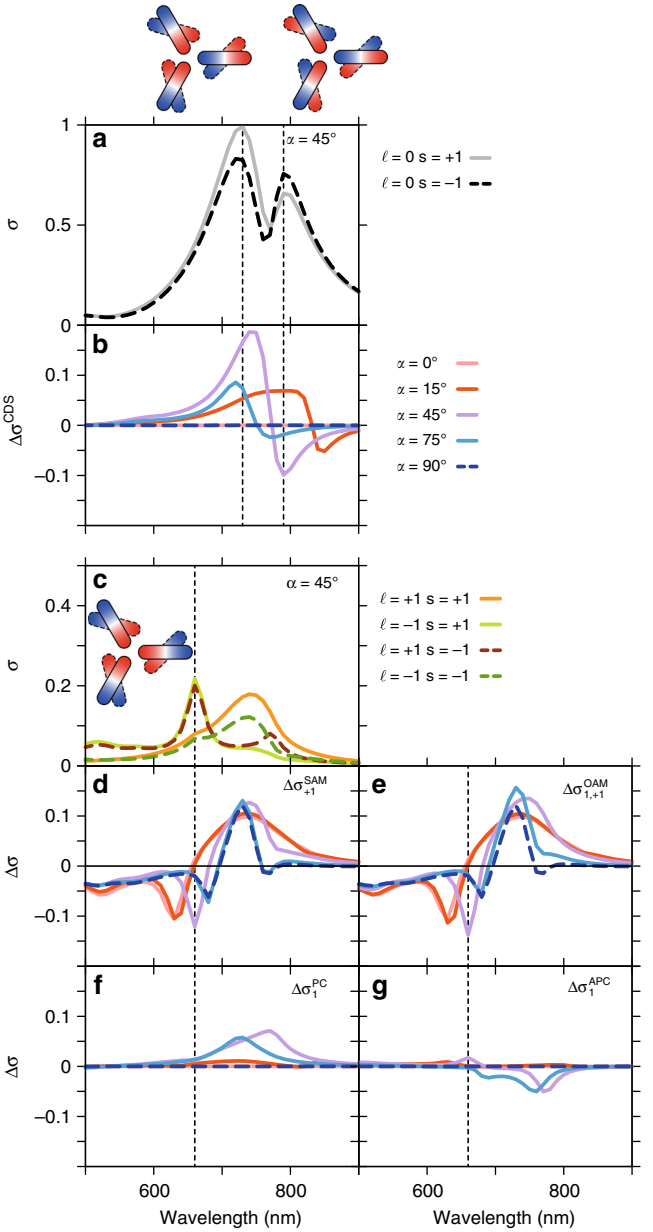

Fig. 4 Dichroism in the trimer. Scattering cross-section spectrum for an angle $\alpha = 45°$ for beams with $\ell = 0$ and $s = \pm 1$ (**a**) and circular differential scattering $\Delta\sigma^{\mathrm{CDS}}$ (**b**). Scattering cross-section spectrum for an angle $\alpha = 45°$ for Bessel beams with $\ell = \pm 1$ and $s = \pm 1$ (**c**). Spectra of several dichroisms as indicated: Spin angular momentum (SAM) dichroism $\Delta\sigma_{+1}^{\mathrm{SAM-D}}$ for $\ell = 1$ (**d**), the orbital angular momentum (OAM) dichroism $\Delta\sigma_{1,+1}^{\mathrm{OAM-D}}$ for $s = +1$ (**e**), and the class dichroisms for the parallel class $\Delta\sigma_1^{\mathrm{PC-D}}$ (**f**) and the anti-parallel class $\Delta\sigma_1^{\mathrm{APC-D}}$ (**g**)

modes, which are able to distinguish not only between circularly polarized and OAM light, but further can distinguish between the positive and negative values of the OAM ℓ. Therefore, the dichroic response is determined by both the the SAM and OAM dichroism.

Discussion

In this paper we have investigated dichroism for OAM light. Using a chiral nanostructure composed of elements of two twisted, stacked nanorods, which exhibits a CDS, we have studied if this dichroism can be directly translated to OAM light. While for the monomer (a single element) the light-matter interaction

was very weak, for the dimer (two elements) the dichroic response to circularly polarized light could be readily transferred to OAM light. When increasing the number of elements to three, the structure is able to distinguish between the two signs of OAM. We showed that an OAM induced dichroism on the same order of the SAM induced dichroism can be obtained. Using the example of a chiral nanostructure, our results show that a strong SAM-D does not necessarily result in a strong OAM-D. Only when a structure is sensitive to the sign of orbital angular momentum, an OAM induced dichroism takes place and structures can be sorted by the OAM.

In addition to the SAM-D and the OAM-D, we introduced a new type of dichroism depending on the class of OAM light. In this class-D a pronounced difference within the same class of OAM light has been found in the scattering spectra. The definitions of dichroism can be also used for helicity dependent absorption as a generalization of the circular dichroism. Our study provides a definition of dichroism for OAM light and a firm foundation for future works, which enables progress in the field of optical manipulation on the nanoscale[49], chiroptical spectroscopy[50] and information technologies by encoding information with higher densities[20] using the combination of OAM and dichroism.

Code availability. The code of the Matlab BEM package is available from Hohenester & Trügler[46].

Data availability

The data that support the findings of this study are available from the corresponding author uopn reasonable request.

Received: 6 July 2018 Accepted: 7 November 2018
Published online: 03 December 2018

References

1. Atkins, P. & Barron, L. Rayleigh scattering of polarized photons by molecules. *Mol. Phys.* **16**, 453–466 (1969).
2. Andrews, D. & Thirunamachandran, T. A quantum electrodynamical theory of differential scattering based on a model with two chromophores i. differential rayleigh scattering of circularly polarized light. *Proc. R. Soc. Lond. A* **358**, 297–310 (1978).
3. Barron, L. D. *Molecular Light Scattering and Optical Activity* (Cambridge University Press, New York, 2009).
4. Berova, N., Di Bari, L. & Pescitelli, G. Application of electronic circular dichroism in configurational and conformational analysis of organic compounds. *Chem. Soc. Rev.* **36**, 914–931 (2007).
5. Fasman, G. D. *Circular Dichroism and the Conformational Analysis of Biomolecules* (Springer Science & Business Media, New York, 2013).
6. Lightner, D. A. & Gurst, J. E. *Organic Conformational Analysis and Stereochemistry from Circular Dichroism Spectroscopy*, vol. 23 (John Wiley & Sons, New York, 2000).
7. Fan, Z. & Govorov, A. O. Plasmonic circular dichroism of chiral metal nanoparticle assemblies. *Nano Lett.* **10**, 2580–2587 (2010).
8. Smith, K. W. et al. Chiral and achiral nanodumbbell dimers: the effect of geometry on plasmonic properties. *ACS Nano* **10**, 6180–6188 (2016).
9. Valev, V. et al. Plasmonic ratchet wheels: switching circular dichroism by arranging chiral nanostructures. *Nano Lett.* **9**, 3945–3948 (2009).
10. Oh, S. S., Demetriadou, A., Wuestner, S. & Hess, O. On the origin of chirality in nanoplasmonic gyroid metamaterials. *Adv. Mater.* **25**, 612–617 (2013).
11. Oh, S. S. & Hess, O. Chiral metamaterials: enhancement and control of optical activity and circular dichroism. *Nano Converg.* **2**, 24 (2015).
12. Wang, Y. et al. Plasmonic chirality of l-shaped nanostructure composed of two slices with different thickness. *Opt. Express* **24**, 2307–2317 (2016).
13. Wang, X. & Tang, Z. Circular dichroism studies on plasmonic nanostructures. *Small* **13** 1601115 (2017).
14. Kang, L., Ren, Q. & Werner, D. H. Leveraging superchiral light for manipulation of optical chirality in the near-field of plasmonic metamaterials. *ACS Photonics* 4, 1298–1305 (2017).
15. Hentschel, M., Schäferling, M., Weiss, T., Liu, N. & Giessen, H. Three-dimensional chiral plasmonic oligomers. *Nano Lett.* **12**, 2542–2547 (2012).
16. Lu, X. et al. Circular dichroism from single plasmonic nanostructures with extrinsic chirality. *Nanoscale* **6**, 14244–14253 (2014).
17. Andrews, D. L. *Structured Light and Its Applications*. (Academic Press, Burlington, MA, 2008).
18. Allen, L., Beijersbergen, M. W., Spreeuw, R. & Woerdman, J. Orbital angular momentum of light and the transformation of laguerre-gaussian laser modes. *Phys. Rev. A* **45**, 8185 (1992).
19. Bozinovic, N. et al. Terabit-scale orbital angular momentum mode division multiplexing in fibers. *Science* **340**, 1545 (2013).
20. Ren, H., Li, X., Zhang, Q. & Gu, M. On-chip noninterference angular momentum multiplexing of broadband light. *Science* **352**, 805 (2016).
21. Mirhosseini, M. et al. High-dimensional quantum cryptography with twisted light. *New J. Phys.* **17**, 033033 (2015).
22. Quinteiro, G. F., Reiter, D. E. & Kuhn, T. Formulation of the twisted-light-matter interaction at the phase singularity: the twisted-light gauge. *Phys. Rev. A* **91**, 033808 (2015).
23. Babiker, M., Bennett, C., Andrews, D. & Romero, L. D. Orbital angular momentum exchange in the interaction of twisted light with molecules. *Phys. Rev. Lett.* **89**, 143601 (2002).
24. Quinteiro, G. F., Schmidt-Kaler, F. & Schmiegelow, C. T. Twisted-light–ion interaction: the role of longitudinal fields. *Phys. Rev. Lett.* **119**, 253203 (2017).
25. Zurita-Sánchez, J. R. & Novotny, L. Multipolar interband absorption in a semiconductor quantum dot. i. electric quadrupole enhancement. *J. Opt. Soc. Am. B* **19**, 1355–1362 (2002).
26. Zurita-Sánchez, J. R. & Novotny, L. Multipolar interband absorption in a semiconductor quantum dot. ii. magnetic dipole enhancement. *J. Opt. Soc. Am. B* **19**, 2722–2726 (2002).
27. Köksal, K. & Koç, F. The effect of twisted light on the ring-shaped molecules: the manipulation of the photoinduced current and the magnetic moment by transferring spin and orbital angular momentum of high frequency light. *Comput. Theor. Chem.* **1099**, 203–208 (2017).
28. Kuzyk, A. et al. Reconfigurable 3d plasmonic metamolecules. *Nat. Mat.* **13**, 862–866 (2014).
29. Auguié, B., Alonso-Gómez, J. L., Guerrero-Martnez, A. & Liz-Marzán, L. M. Fingers crossed: optical activity of a chiral dimer of plasmonic nanorods. *J. Phys. Chem. Lett.* **2**, 846–851 (2011).
30. Yin, X., Schäferling, M., Metzger, B. & Giessen, H. Interpreting chiral nanophotonic spectra: the plasmonic Born–kuhn model. *Nano Lett.* **13**, 6238–6243 (2013).
31. Wang, L.-Y. et al. Circular differential scattering of single chiral self-assembled gold nanorod dimers. *ACS Photonics* **2**, 1602–1610 (2015).
32. Yin, X. et al. Active chiral plasmonics. *Nano Lett.* **15**, 4255–4260 (2015).
33. Najafabadi, A. F. & Pakizeh, T. Analytical chiroptics of 2d and 3d nanoantennas. *ACS Photonics* **4**, 1447–1452 (2017).
34. Jáuregui, R. Rotational effects of twisted light on atoms beyond the paraxial approximation. *Phys. Rev. A* **70**, 033415 (2004).
35. Quinteiro, G. F. & Kuhn, T. Light-hole transitions in quantum dots: Realizing full control by highly focused optical-vortex beams. *Phys. Rev. B* **90**, 115401 (2014).
36. Saleh, B. E. A. & Teich, M. C. *Fundamentals of Photonics* (Wiley, New York, 2007).
37. Kerber, R. M., Fitzgerald, J. M., Reiter, D. E., Oh, S. S. & Hess, O. Reading the orbital angular momentum of light using plasmonic nanoantennas. *ACS Photonics* **4**, 891–896 (2017).
38. Zambrana-Puyalto, X., Vidal, X. & Molina-Terriza, G. Angular momentum-induced circular dichroism in non-chiral nanostructures. *Nat. Commun.* **5**, 4922, (2014).
39. Wang, S. et al. Angular momentum-dependent transmission of circularly polarized vortex beams through a plasmonic coaxial nanoring. *IEEE Photonics J.* **10**, 1–9 (2018).
40. Araoka, F., Verbiest, T., Clays, K. & Persoons, A. Interactions of twisted light with chiral molecules: an experimental investigation. *Phys. Rev. A* **71**, 055401 (2005).
41. Löffler, W., Broer, D. & Woerdman, J. Circular dichroism of cholesteric polymers and the orbital angular momentum of light. *Phys. Rev. A* **83**, 065801 (2011).
42. Forbes, K. A. & Andrews, D. L. Optical orbital angular momentum: twisted light and chirality. *Opt. Lett.* **43**, 435–438 (2018).
43. Brullot, W., Vanbel, M. K., Swusten, T. & Verbiest, T. Resolving enantiomers using the optical angular momentum of twisted light. *Sci. Adv.* **2**, e1501349 (2016).
44. Rothemund, P. W. Folding DNA to create nanoscale shapes and patterns. *Nature* **440**, 297–302 (2006).
45. Douglas, S. M. et al. Self-assembly of DNA into nanoscale three-dimensional shapes. *Nature* **459**, 414–418 (2009).

46. Hohenester, U. & Trügler, A. Mnpbem–a matlab toolbox for the simulation of plasmonic nanoparticles. *Comput. Phys. Commun.* **183**, 370 (2012).
47. Johnson, P. B. & Christy, R.-W. Optical constants of the noble metals. *Phys. Rev. B* **6**, 4370 (1972).
48. Nordlander, P., Oubre, C., Prodan, E., Li, K. & Stockman, M. I. Plasmon hybridization in nanoparticle dimers. *Nano Lett.* **4**, 899 (2004).
49. Gao, D. et al. Optical manipulation from the microscale to the nanoscale: fundamentals, advances and prospects. *Light Sci. Appl.* **6**, e17039 (2017).
50. Berova, N., Polavarapu, P. L., Nakanishi, K. & Woody, R. W. *Comprehensive Chiroptical Spectroscopy: Applications in Stereochemical Analysis of Synthetic Compounds, Natural Products, and Biomolecules* 2 (John Wiley & Sons, Hoboken, 2012).

Acknowledgements

We gratefully acknowledge the Matlab BEM package provided by A. Trügler and U. Hohenester. R.M. Kerber is grateful for financial support from the German Academic Exchange Service (DAAD). This research was supported by the Engineering and Physical Sciences Research Council UK through the projects EP/L024926/1 and EP/L027151/1. This work is part-funded by the European Regional Development Fund through the Welsh Government.

Author contributions

R.M.K. performed the simulations using the BEM. R.M.K., J.M.F., S.S.O., D.E.R. and O.H. discussed the results and wrote the manuscript.

Additional information

Competing interests: The authors declare no competing interests.